CHEMISTRY OF MATERIALS

Article

pubs.acs.org/cm

Combining Coordination Modulation with Acid–Base Adjustment for the Control over Size of Metal–Organic Frameworks

Hailing Guo,[†,§] Yongzhong Zhu,[‡,§] Song Wang,[†] Shengqun Su,[†] Liang Zhou,[†] and Hongjie Zhang[†,*]

[†]State Key Laboratory of Rare Earth Resource Utilization, Changchun Institute of Applied Chemistry, Chinese Academy of Sciences, Changchun, 130022 P.R. China

[‡]Education & Research (Chemistry), German Institute of Science and Technology - TUM Asia, 10 Central Exchange Green, #03-01 Pixel Building, 138649 Singapore

Supporting Information

ABSTRACT: Precise control over size and morphology of metal–organic frameworks (MOFs) is challenging but important for extending these hybrid materials to many more advanced applications, in particular for nanotechnology and device integration. Through studying parameters for the fabrication of nanosized Dy(BTC)(H_2O) MOF crystals using sodium acetate as the modulator, this paper discloses two essential parameters for miniaturizing the size of MOF crystals to the nanometer scale. One is the proper acid–base environment of the reaction medium which governs deprotonation of the organic linker and, hence, the nucleation process. The other is the use of capping groups capable of inhibiting crystallites from growing. Combining these two parameters makes it possible to control the size and change the morphology of Dy(BTC)(H_2O) crystals. A mechanism based on coordination modulation together with pH adjustment is proposed for the growth of nanosized MOF crystals.

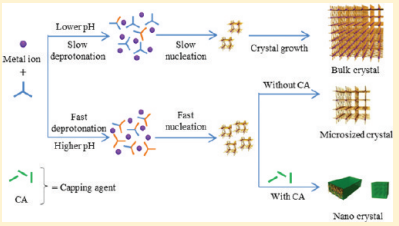

KEYWORDS: *metal–organic frameworks, coordination modulation, crystal growth, nucleation, nanocrystals*

INTRODUCTION

Metal–organic frameworks (MOFs) or porous coordination polymers (PCPs) represent a novel class of porous inorganic–organic materials which are built from metal ions and organic linkers.[1−5] Their varying structure and well-defined porosity together with their tunable functionality make them extremely attractive for applications such as gas adsorption and storage,[6−8] drug release,[9−11] sensing,[12] membranes,[13,14] and in catalysis.[15,16] Previous research focused more on the design, synthesis, characterization, and application of bulk MOFs materials; however, some applications of MOFs depend not only on the ability to control the chemical structure of a material but also its microstructure, size, and morphology. For example, the processing of MOFs into high quality films or membranes requires the precise control over size and orientation of individual MOF crystal.[13,14,17] It is reported that the kinetics of methanol adsorption increases dramatically over nanoparticles although the overall adsorption capacities of nanoparticles and bulk crystals are almost identical.[18] Likewise, miniaturizing the size of MOF crystals is beneficial for improving its catalytic activity.[19] All in all, tailored fabrication of well-defined MOF crystallites in the submicrometer size regime is highly desirable.

To date, several strategies have been utilized for the synthesis of nanosized MOFs (NMOFs). Mirkin et al. described a method for preparing micro-or submicrometer-scale spherical particles of zinc-based MOF crystals simply by adding an initiation solvent to a precursor solution containing metal ions and metalloligands.[20] Making use of a reverse microemulsion system, Lin et al. reported the synthesis of several different types of NMOFs for multimodal imaging,[21] magnetic resonance imaging,[22] and drug delivery.[9−11] Masel et al. demonstrated that nanosized isoreticular metal–organic frameworks (IRMOFs) could be synthesized within a minute with assistance of microwave irradiation.[23] NMOFs were synthesized under ultrasound irradiation as well.[24] Assisted with the bridging ligand, nanocystals of a prototypical zeolitic imidazole framework (ZIF) material, ZIF-8, were fabricated in either methanol[25,26] or water[27] solution.

Recently, the coordination modulation method, which is a well-established method for fabrication of metal or semiconductor nanoparticles,[28,29] was adapted for the fabrication of NMOFs.[30−35] For example, Fischer et al.[30]selected *p*-perfluoromethylbenzenecarboxylate as the capping agent to grow MOF-5 nanocrystals; Kitagawa et al.[31] used a rather simple monocarboxylic acid, acetic acid, for the fabrication of a MOF nanorods, and meanwhile Ferey et al.[33] directly utilized iron(III) acetate as metal source for the formation of MIL-89 colloidal solution. This method utilized the strategy of modulating the coordination equilibrium by adding capping agents with the same chemical functionality as the linkers to adjust the coordination interactions between metal ions and organic linkers, and thus, the rate of framework extension and crystal growth, and finally allows the control over the size and morphology of the resulting crystals. Inspired by these achievements, NMOFs containing one or two lanthanide

Received: May 31, 2011
Revised: December 1, 2011
Published: December 20, 2011

metal(s) were successful prepared by us using carboxylate salts as the capping agent.[32] Furthermore, continuous, smooth, and mechanical stable $Eu_{1-x}Tb_x$MOF membranes exhibiting fascinating luminescent properties were fabricated by spin coating technology. More recently, Behrens et al.[34] reported the synthesis of isoreticular Zr-MOFs by the addition of acetic and benzoic acid as coordination modulator. Wiebcke et al.[35] disclosed that nanosized ZIF-8 could be prepared by employing an excess of the bridging didentate ligand and various simple auxiliary monodentate ligands with different chemical functionalities (carboxylate, *N*-heterocycle, alkylamine). The functionality of the monodentate ligands was ascribed to the modulation effect of modulator on complex formation and deprotonation equilibia during crystal nucleation and growth. A close check on the coordination method revealed that results from various research groups[30−33] suggested that the coordination method is promising for creation of nanosized MOFs and acetic ion is a good capping candidate. However, bulk crystals instead of expected nanocrystals formed when acetic acid was used for the synthesis of Dy(BTC)H_2O (BTC = 1,3,5-benzenetricarboxylic acid) (this work). Kitagawa et al. also found that acetic acid was effective for the synthesis of nanosized HKUST-1 only when combined with microwave radiation.[36] The confusing results obtained with acetic acid suggest that there must be other parameters which play an equally important role for miniaturizing the size of MOF crystals. Figuring out these parameters is helpful and important to understand and generalize the coordination modulation method for the synthesis of NMOFs.

In a previous communication,[32] we reported a simple and straightforward method for the synthesis of Dy(BTC)H_2O nanocrystals using sodium carboxylates as the capping agent. However, the key fabrication parameters were not identified and the chemistry behind was not revealed in detail. In this paper, the influence of nanoparticle fabrication parameters such as amount and type of capping agents and the pH of the reaction medium was studied. The aim is to understand the essence of MOF nucleation and the crystal growth process. A general mechanism for the formation of NMOFs was proposed. The proposed mechanism proved applicable for the syntheses of other types of MOF nanocrystals like MOF-5 and HKUST-1.

EXPERIMENTAL SECTION

Materials and Chemicals. Dysprosium(III) nitrate hydrate ($Dy(NO_3)_3{\cdot}xH_2O$, copper(II) nitrate trihydrate ($Cu(NO_3)_2{\cdot}3H_2O$), zinc acetate dihydrate ($Zn(CH_3COO)_2{\cdot}2H_2O$), acetic acid ($CH_3COOH$), *N*,*N*-dimethylformamide (DMF), and sodium acetate anhydrous (CH_3COONa) were purchased from Sinopharm Chemical Reagent Co., Ltd. 1,3,5-Benzenetricarboxylic acid (BTC) was purchased from Fluka. Triethyl amine was obtained from Aldrich. All chemicals were used without further purification.

Preparation of Dy(BTC)H_2O) Bulk Crystals. Bulk Dy(BTC)H_2O) crystals were synthesized following Qiu et al.[37] with slight modification. In a typical synthesis, $Dy(NO_3)_3{\cdot}xH_2O$ (60 mg, 0.13 mmol) and BTC (20 mg, 0.1 mmol) were dissolved in 8 mL of DMF and 2 mL of deionized water at ambient temperature (~25 °C). This mixture was defined as the standard solution (no precipitation was observed even after this solution was kept at room temperature for several weeks). The crystallization was performed at 60 °C under static conditions. After 72 h, the resulting transparent bulk crystals were recovered by filtration.

Preparation of Dy(BTC)(H_2O) Nanocrystals Using Sodium Acetate. To the standard solution was added 0−5 equiv of sodium acetate with respect to BTC under stirring. After 10 min, the pH value of the solution was measured and then was kept undisturbed in an oven at 60 °C for 0−48 h. After cooling down, the pH value of the mixture was measured again. The product was isolated by repeated centrifugation and washing with DMF. The resulting solid was dried overnight at room temperature before further analysis.

Preparation of Dy(BTC)(H_2O) Crystals Using Other Additives. To the standard solution was added 0.1−0.5 mmol acetic acid, 0.3 mmol sodium nitrate, or 0.1−0.5 mmol TEA separately . The crystallization was performed at 60 °C for 24 h. The washing and drying procedures were the same as before.

Preparation of Dy(BTC)(H_2O) Nanocrystals Using HAc+TEA. To the standard solution was added 2−5 equiv of acetic acid with respect to BTC. After mixing well, the pH value of the solution was adjusted to around 5.9 with TEA. The crystallization was performed at 60 °C for 24 h. The washing and drying procedures were the same as before.

Preparation of HKUST-1 (Cu(BTC)) Nanocrystals. A solution of $Cu(NO_3)_2{\cdot}3H_2O$ (0.362 g, 1.5 mmol) and BTC (0.168, 0.8 mmol) was prepared by dissolving them in a water/ethanol (10 mL/10 mL) solution. To this solution was added sodium acetate (0−0.24 mmol), and a milky colloidal solution was formed immediately. Subsequently, the milky colloidal solution was transferred to a Teflon lined autoclave to allow crystal growth at 120 °C for 3 days. After crystallization, the product was isolated by repeated centrifugation and washing with ethanol.

Preparation of MOF-5 Nanocrystals. Two solutions prepared separately by dissolving terephthalic acid (66 mg, 0.4 mmol) in 7.5 mL of DMF and $Zn(CH_3COO)_2{\cdot}2H_2O$ (88−220 mg, 0.4−1 mmol) in 7.5 mL of DMF were mixed and stirred at ambient temperature for 4−24 h. The resulting suspension was isolated by repeated centrifugation and washing with DMF.

Characterization. The powder X-ray diffraction (PXRD) patterns were collected on a Siemens D5005 diffractometer (in reflection mode) with Cu Kα radiation (λ = 1.5406 Å) with a scan speed of 4 s/step and a step size of 0.02°. The simulated pattern was obtained from single-crystal X-ray analysis. The size and morphology of samples were characterized using field-emission scanning electron microscopy (FE-SEM, Hitachi S4800) at an accelerating voltage of 10 kV and a transmission electron microscope (TEM) at an operation voltage of 200 kV (JEOL JSM-3010). The infrared spectrum (IR) was collected on a NEXUS FT-IR using the KBr technique. Thermal gravimetric analysis (TGA) was performed on a Perkin-Elmer TGA thermogravimetric analyzer in the temperature range of 25−800 °C under nitrogen atmosphere, at a heating rate of 10 °C/min. N_2 adsorption/desorption isotherms were recorded at −196 °C on an ASAP 2020 instrument. Before measurement, samples were degassed at 200 °C overnight.

RESULTS AND DISCUSSION

Carboxylate salts such as sodium acetate and sodium formate are effective capping agents in reducing the size of Dy(BTC)-H_2O crystals from micrometer to nanometer, which has been disclosed by us.[32] In the present study, in order to understand how carboxylate salts affect the crystallization process, the effect of sodium acetate was studied by altering the concentration of sodium acetate (given below as equivalent with respect to BTC) in the synthesis solution. In the absence of sodium acetate, the standard solution remained transparent at ambient temperature even after several weeks. In the presence of 1 equiv of sodium acetate, the solution became cloudy within several minutes while 3 equiv led to colloidal solution within a minute. When sodium acetate exceeded 3.5 equiv, white precipitate formed immediately. These observations clearly indicate that an increase of the sodium acetate significantly accelerated the particle formation rate. SEM images (Figure 1) show that, with addition of 1 equiv of sodium acetate, the length of rod-like crystals decreases significantly from the original 40−60 μm (see ref 32) to around 3 μm (Figure 1a). Two equivalents of sodium

dx.doi.org/10.1021/cm202593h | *Chem. Mater.* 2012, 24, 444−450

acetate lead to rod-like submicrocrystals with decreasing aspect ratio (Figure 1b). The spherical monodisperse nanocrystals with average size of 71 nm (Figure 1c, statistic particle size distribution in Supporting Information Figure S2) are obtained in the presence of 3 equiv of sodium acetate. However, the particle size increased again when the amount of the sodium acetate was more than 3.5 equiv (Figure 1d–f). In such a case, the increase in particle size could be resulted from further growth via aggregation of small nuclei or nanoparticles which formed extremely fast in the presence of a large amount of sodium acetate.

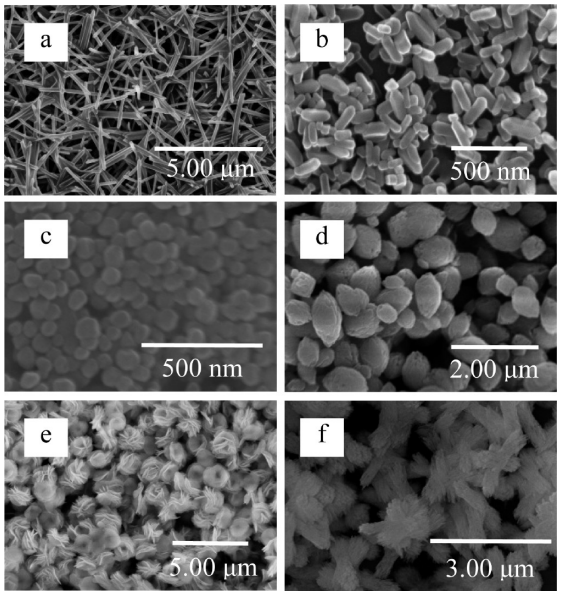

Figure 1. SEM images of Dy(BTC)H_2O synthesized with different amounts of sodium acetate: (a) 1, (b) 2, (c) 3, (d) 3.5, (e) 4, and (f) 5 equiv.

Table 1. pH Value of Synthesis Mixtures before and after Crystallization[a]

equiv of sodium acetate	pH_1	pH_2	pH increase (%)
0	3.6	5.4	50
1	4.4	5.9	34
3	5.8	6.8	17
3.5	6.5	7.1	10
4	7.2	7.8	8
5	7.9	8.1	3

[a] pH_1 and pH_2 are the pH values before and after crystallization at 60 °C.

Since sodium acetate is a base (pk_b = 9.25), which can facilitate the deprotonation of the organic linker BTC, it is deducible that the regulation effect, to some degree, is related to the acid–base environment of the synthesis system. To clarify this, pH values of the reaction mixtures were measured, and the results are summarized in Table 1 (the use of pH was on the boundary conditions in our organic–water solvent system, but it helped for us to understand the chemistry that occurred). It was found that the standard solution had a value of 3.6 before crystallization. At such low pH, the concentration of deprotonated BTC was very low, making the formation of Dy(BTC)H_2O MOF crystals nearly impossible. After heating at 60 °C for 48 h, the pH increased to 5.4 due to the formation of

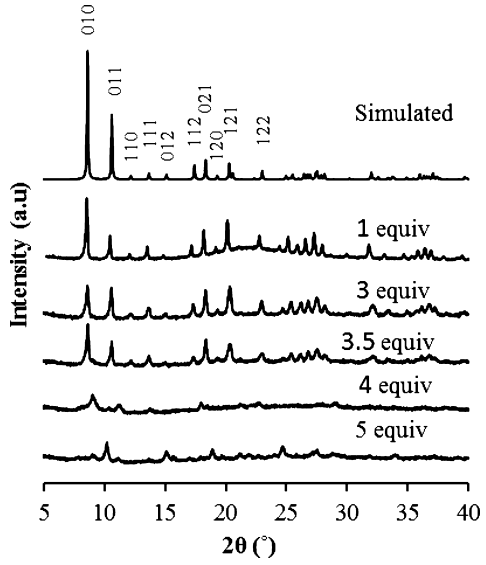

Figure 2. XRD patterns of Dy(BTC)H_2O synthesized with different amounts of sodium acetate (given as equivalents with respect to BTC).

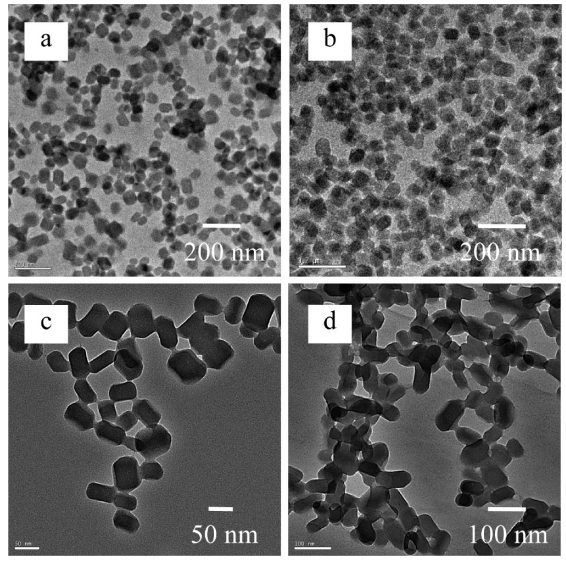

Figure 3. TEM images of Dy(BTC)(H_2O) synthesized with addition of 3 equiv of sodium but at different synthesis conditions: after (a) 10 min stirring at room temperature, (b) 10 min at 60 °C, (c) 30 min at 60 °C, and (d) 24 h at 60 °C.

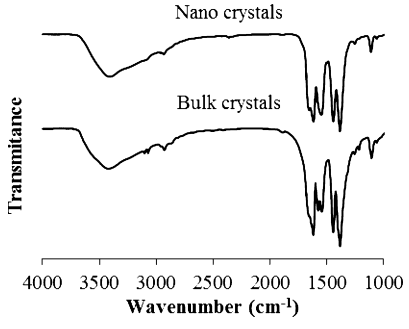

Figure 4. IR spectra of Dy(BTC)H_2O bulk and nanocrystals. Nanocrystals were synthesized with addition of 3 equiv of sodium acetate.

dx.doi.org/10.1021/cm202593h | Chem. Mater. 2012, 24, 444–450

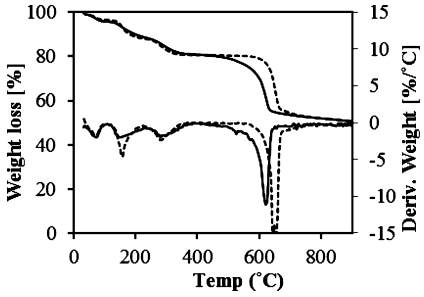

Figure 5. TGA/DTA of Dy(BTC)(H_2O) bulk (dashed line) and nanocrystals (solid line). The top two curves are the TGA result and the bottom two lines the DTA result. Nanocrystals were synthesized with addition of 3 equiv of sodium acetate.

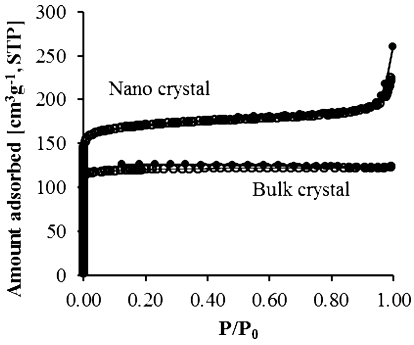

Figure 6. N_2 adsoption/desorption isotherms of Dy(BTC)(H_2O) bulk and nanocrystals at 77 K. Adsorption data are shown as open circles and desorption data as closed circles. Nanocrystals were synthesized with addition of 3 equiv of sodium acetate.

dimethyl amine, a Brønsted base formed by the Dy^{3+}-catalyzed decomposition of DMF. As the formation rate of dimethyl amine was rather low at this temperature, only bulk crystals were formed. Upon addition of a different amount of the sodium acetate, the pH of the synthesis solutions increased accordingly and was higher than that of the standard solution. At higher pH value, more deprotonated BTC ions were available for coordination with metal ions, resulting in

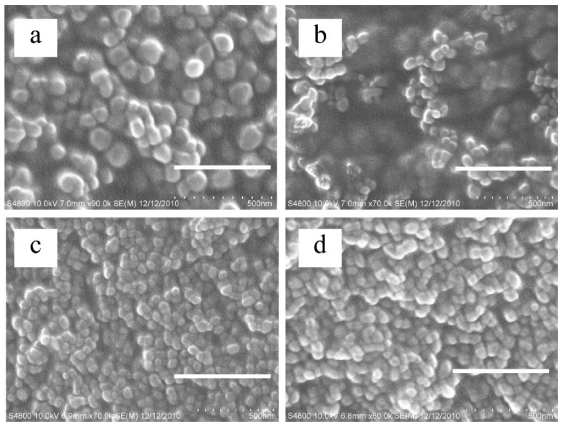

Figure 7. SEM images of Dy(BTC)H_2O nanocrystals synthesized with addition of both acetic acid (given as equivalent with respect to BTC) and TEA: (a) 2, (b) 3, (c) 4, and (d) 5 equiv of acetic acid. The pH of all solutions was adjusted to around 5.9 using TEA. Crystallization was performed at 60 °C for 24 h. All scale bars represent 500 nm.

increasingly accelerated nucleation rates and therefore decreasing crystal size and crystal anisotropy (Figure 1). Particle sized decreased and fell within the nano range (<100 nm) at pH around 5.8 (value before heating). However, large particles formed when pH was higher than pH = 6.5, and amorphous materials (proved by XRD analysis) were obtained when the pH was higher than 7.2. Nevertheless, the size and morphology of particles could be tuned through altering the amount of sodium acetate. As higher pH leads to higher nucleation rate, one may expect formation of nanocrystals even in the absence of a capping agent because growth may stop due to rapid decrease of supersaturation. To verify this assumption, a set of experiments was performed by adding varying amounts of TEA (an organic base) to the standard solution. Although smaller crystal size (down to several micrometers) could be obtained, the formation of nanosized Dy(BTC)H_2O crystals was never observed (Supporting Information Figure S1). Therefore, adjusting only the basicity is not effective enough to form

Scheme 1. Proposed Dy(BTC)H_2O Crystal Formation Mechanism[a]

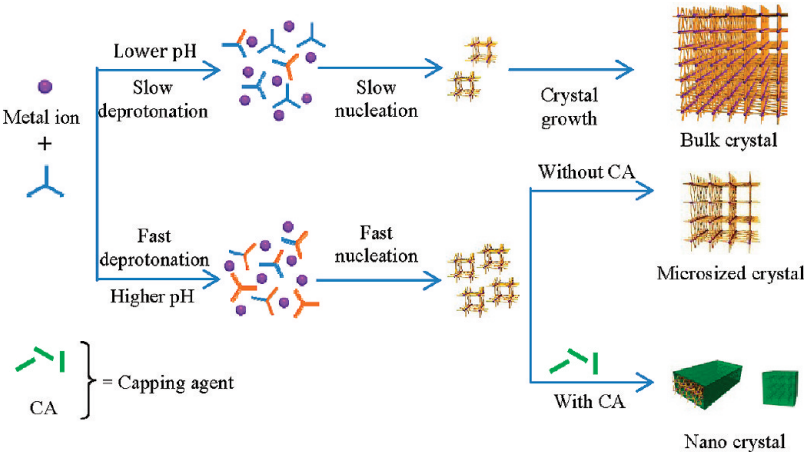

[a]Blue and orange colors represent protonated and deprotonated COO− groups in organic linker. At lower pH value, both deprotonation of organic linker BTC and nucleation are slow, eventually leading to bulk crystals. On the contrary, deprotonation and nucleation are faster at higher pH. In the presence of capping agent, crystal growth is restricted, resulting in nanocrystals. In more basic medium but without capping agent, the nuclei formation rate is fast but the nuclei growth is not restricted; thus, microsized crystals are obtained.

dx.doi.org/10.1021/cm202593h | *Chem. Mater.* 2012, 24, 444–450

nanocrystals; capping groups are still needed, at least in the synthesis of Dy(BTC)H_2O nanocrystals.

The structure of samples was further studied by X-ray powder diffraction (XRPD). As shown in Figure 2, samples with up to 3.5 equiv of sodium acetate show diffraction patterns identical to those of the simulated one, indicating that the structure of Dy(BTC)H_2O is well preserved. Remarkably, the broadening of the reflections is observed, suggesting the formation of smaller crystals. With addition of more than 4 equiv of sodium acetate, nearly all characteristic diffraction peaks of Dy(BTC)H_2O disappear and the synthesized materials become amorphous. It is believed that the competition of capping groups and organic linkers for coordination to metal ions and the extremely fast agglomeration rate prevent the assembly of small nuclei or clusters from formation of ordered structures. The XRD study indicates that the structure of Dy(BTC)H_2O is not affected by moderate amounts of sodium acetate; however, it could be altered by a large amount of sodium acetate (>4 equiv).

Insight into the nucleation and crystal growth of Dy(BTC)-H_2O was obtained by analyzing the TEM images taken after different crystallization times. The ratio between sodium acetate and BTC was fixed at 3. This ratio ensured that equal amounts of carboxylate groups resulted from the capping agent and network builder. As shown in Figure 3, in the presence of sodium acetate, monodisperse nanoparticles with average size of 55 nm were observed by TEM (Figure 3a, particle size distribution in Supporting Information Figure S3a) after 10 min reaction at room temperature. Some particles exhibited already sharp edges, implying their crystalline features. Indeed, XRD of the centrifuged sample confirmed this point (Supporting Information Figure S4). After 10 min of crystallization at 60 °C, no significant difference was observed in particle size (Figure 3b), but the size distribution was narrower (Supporting Information Figure S3b). After 30 min of crystallization, the shape of the particles became more regular (Figure 3c). At the same time, the morphology of particles shifted from almost square to slightly rectangular shape, implying that anisotropy is developing during crystal growth but the further growth is prohibited by the capping agent because no obvious increase in crystal size was observed even though the crystallization time increased to 24 h, implying that nanocrystals were quite stable once formed at ambient temperature.

Combining time-resolved light scattering and SEM study, Fischer et al. proposed two limiting mechanisms for the formation of MOF particles.[38] In one case, nucleation occurs within an initiation period in the supersaturated solution. This nucleation burst is succeeded by a relatively slow phase of particle growth, leading to particles with a narrow size distribution. The growth of MOF-5 nanocrystals was claimed to follow this limiting case. In another case, a relatively slow nucleation process is followed by extremely fast particle growth. Since nucleation extends over a long period of time, the spectrum of particle distribution becomes comparatively broad. The formation of HKUST-1 nanoparticles is compatible with this mechanism. Considering the fast Dy(BTC)H_2O nucleation and particle growth process modulated by sodium acetate together with an extremely narrow particle size distribution, the growth of Dy(BTC)H_2O is believed to be following the first mechanism.

IR spectroscopy was used to characterize functional groups in bulk and nanocrystals. As revealed in Figure 4, both samples exhibit the characteristic asymmetric stretching vibrations of carboxylate groups in the range 1590−1480 cm^{-1} and the symmetric vibrations centered at 1381 cm^{-1}.[39,40] This observation is in good agreement with the stretching vibration of carboxylate groups in the IR spectrum of Dy(BTC)·5H_2O ($\nu_{as(COO-)}$ at 1556 cm^{-1} and $\nu_{s(COO-)}$ at 1381 cm^{-1}).[40] Surprisingly, the bulk crystals exhibit two bands, centered at 1573 cm^{-1} and 1541 cm^{-1}, respectively, in the asymmetric stretching vibration range of the COO groups whereas the nanocrystals seem to have only one relatively strengthened band centered at 1550 cm^{-1}. The appearance of only one asymmetric vibration band in the nanocrystals is tentatively ascribed to the overlap of the asymmetric vibration of the surface acetate groups and the framework carboxylate groups of BTC. However, in the same wavenumber range, the vibration band could also be resulted from the stretching vibrations of the benzene ring as well as deformation vibration of water molecules.[40] Beside bands related to COO− groups, the band at 1441 cm^{-1} is ascribed to the C−C vibration in the aromatic ring. The presence of water molecules is confirmed by a broad band in the region 3649−2960 cm^{-1} and a sharp band centered at 1612 cm^{-1}. The former band originates from stretching vibrations of OH groups from water molecules while the latter is due to the water bending vibration. The absence of characteristic absorption bands of free BTC at1730−1690 cm^{-1} and at 1280 cm^{-1}, due to the stretching vibration of the C═O group and the C−OH group, respectively, indicates that BTC is completely deprotonated after crystallization.[41]

Typical TGA/DTA curves of bulk and nanocrystals are shown in Figure 5. The two samples have similar TGA/DTA curves up to 400 °C. The weight loss below 100 °C is due to desorption of physisorbed water, while the weight loss in the temperature range 130−220 °C arises from the occluded solvent DMF and/or water. The third weight loss at temperatures between 220 and 350 °C is associated with the release of coordinated water molecules and/or DMF which could be identified by analysis of the evolved gases. The remarkable difference between nanocrystals and bulk crystals appears in the temperature range 410−680 °C. In this region, the dramatic weight loss comes from the decomposition of organic linkers in the framework. Nanocrystals decompose slowly by releasing CO_2 starting at ∼410 °C and ending at ∼650 °C, whereas bulk crystals start to release CO_2 at higher temperature, ∼500 °C, and up to ∼675 °C. TGA/DTA combined with mass spectrometric analysis shows that nanocrystals are not as stable as bulk crystals. Given their size difference, this result is not unexpected.

N_2 adsorption/desorption isotherms of bulk and nanocrystals are shown in Figure 6. Both samples show a type I sorption isotherm typical for microporous materials. Nanocrystals have a BET surface area of 574 $m^2\ g^{-1}$, much higher than that of the bulk crystals (403 $m^2\ g^{-1}$), indicating that the decrease in crystal size from bulk to nanoscale has a significant effect on surface area. The increased surface area is believed to be related to the higher external surface area of nanocrystals.

On the basis of our study, a mechanism for the formation of Dy(BTC)(H_2O) nanocrystals was proposed (Scheme 1). This mechanism is similar to a general scheme plotted by Kitagawa et al.[31] but in more detail. In this mechanism, two critical points are (1) appropriate acid−base reaction medium capable of adjusting deprotonation and nucleation rate and (2) effective capping agent being able to compete with the organic link for the coordination to metal ions. According to this mechanism, acetic acid definitely can be used as a capping agent for the

dx.doi.org/10.1021/cm202593h | Chem. Mater. 2012, 24, 444−450

synthesis of Dy(BTC)(H_2O) nanocrystals on the condition that a suitable acid–base reaction medium is provided. Indeed, using TEA as pH mediator to adjust pH to around 5.9, we were able to obtain Dy(BTC)(H_2O) nanocystals using acetic acid as the capping agent (Figure 7). Remarkably, spherical monodisperse nanocystals with sizes in the range 50–85 nm (particle size distribution in Supporting Information Figure S5) were prepared over a wide range of acetic acid to BTC ratios (acetic acid/BTC = 2–5) while the Dy(BTC)(H_2O) structure was not affected (Supporting Information Figure S6). It was noticed that the sizes of particles are slightly smaller with more acetic acid, indicating the capping effect of acetic groups. Following this mechanism, nanosized MOF-5 (Supporting Information Figure S7) and HKUST-1 (Supporting Information Figure S8) crystals were obtained in a similar manner as well, proving that the mechanism is extendable and applicable to the synthesis of other types of NMOF crystals. It is worth mentioning that the coordination and deprotonation function of modulating ligands were reported to be significant also for the synthesis of ZIF-8 nanocrystals.[35]

In summary, the effects of the sodium acetate on modulating nucleation and crystal growth process to form nanosized Dy(BTC)H_2O crystals were explored in detail. The size of Dy(BTC)H_2O crystals can be controlled from micrometer to nanometer simply by altering the amount of the sodium acetate added to the synthesis solution. However, too much sodium acetate may lead to amorphous materials. The rate of crystal growth was significantly accelerated by the sodium acetate. The enhancing effect is related to the basicity of the sodium acetate which can greatly prompt the deprotonation rate of the organic linkers and hence the nucleation rate.

■ ASSOCIATED CONTENT

Ⓢ Supporting Information

SEM images, particle size distributions, and

XRD patterns (PDF). This material is available free of charge via the Internet at http://pubs.acs.org.

■ AUTHOR INFORMATION

Corresponding Author

*E-mail: hongjie@ciac.jl.cn.

Author Contributions

[§]These authors contributed equally.

■ ACKNOWLEDGMENTS

The authors are grateful for financial support from the Postdoctoral National Natural Science Foundation of China (Grant Nos. 20090461043), Chinese Academy of science K.C. Wong Postdoctoral fellowships, the National Natural Science Foundation of China (Grant Nos. 20631040, 20602035, and 20610102007) and the MOST of China (Grant Nos. 2006CB601103, 2006DFA42610).

■ REFERENCES

(1) Yaghi, O. M.; O'Keeffe, M.; Ockwig, N. W.; Chae, H. K.; Eddaoudi, M.; Kim, J. *Nature* **2003**, *423* (6941), 705.

(2) Kitagawa, S.; Kitaura, R.; Noro, S. *Angew. Chem., Int. Ed.* **2004**, *43* (18), 2334.

(3) Rao, C. N. R.; Natarajan, S.; Vaidhyanathan, R. *Angew. Chem., Int. Ed.* **2004**, *43* (12), 1466.

(4) Ferey, G. *Chem. Soc. Rev.* **2008**, *37* (1), 191.

(5) Maspoch, D.; Ruiz-Molina, D.; Veciana, J. *Chem. Soc. Rev.* **2007**, *36* (5), 770.

(6) Ma, S.; Sun, D.; Simmons, J. M.; Collier, C. D.; Yuan, D.; Zhou, H.-C. *J. Am. Chem. Soc.* **2007**, *130* (3), 1012.

(7) Furukawa, H.; Ko, N.; Go, Y. B.; Aratani, N.; Choi, S. B.; Choi, E.; Yazaydin, A. O.; Snurr, R. Q.; O'Keeffe, M.; Kim, J.; Yaghi, O. M. *Science* **2010**, *329* (5990), 424.

(8) Mueller, U.; Schubert, M.; Teich, F.; Puetter, H.; Schierle-Arndt, K.; Pastre, J. *J. Mater. Chem.* **2006**, *16* (7), 626.

(9) Taylor-Pashow, K. M. L.; Rocca, J. D.; Xie, Z.; Tran, S.; Lin, W. *J. Am. Chem. Soc.* **2009**, *131* (40), 14261.

(10) Rieter, W. J.; Taylor, K. M. L.; Lin, W. *J. Am. Chem. Soc.* **2007**, *129* (32), 9852.

(11) Rieter, W. J.; Pott, K. M.; Taylor, K. M. L.; Lin, W. *J. Am. Chem. Soc.* **2008**, *130* (35), 11584.

(12) Allendorf, M. D.; Houk, R. J. T.; Andruszkiewicz, L.; Talin, A. A.; Pikarsky, J.; Choudhury, A.; Gall, K. A.; Hesketh, P. J. *J. Am. Chem. Soc.* **2008**, *130* (44), 14404.

(13) Zacher, D.; Shekhah, O.; Woll, C.; Fischer, R. A. *Chem. Soc. Rev.* **2009**, *38* (5), 1418.

(14) Shekhah, O.; Liu, J.; Fischer, R. A.; Woll, C. *Chem. Soc. Rev.* **2011**, *40* (2), 1081.

(15) Lee, J.; Farha, O. K.; Roberts, J.; Scheidt, K. A.; Nguyen, S. T.; Hupp, J. T. *Chem. Soc. Rev.* **2009**, *38* (5), 1450.

(16) Corma, A.; García, H.; Llabrés i Xamena, F. X. *Chem. Rev.* **2010**, *110* (8), 4606.

(17) Morris, R. E. *ChemPhysChem* **2009**, *10* (2), 327.

(18) Tanaka, D.; Henke, A.; Albrecht, K.; Moeller, M.; Nakagawa, K.; Kitagawa, S.; Groll, J. *Nat. Chem.* **2010**, *2* (5), 410.

(19) Park, K. H.; Jang, K.; Son, S. U.; Sweigart, D. A. *J. Am. Chem. Soc.* **2006**, *128* (27), 8740.

(20) Oh, M.; Mirkin, C. A. *Nature* **2005**, *438* (7068), 651.

(21) Rieter, W. J.; Taylor, K. M. L.; An, H.; Lin, W.; Lin, W. *J. Am. Chem. Soc.* **2006**, *128* (28), 9024.

(22) Taylor, K. M. L.; Rieter, W. J.; Lin, W. *J. Am. Chem. Soc.* **2008**, *130* (44), 14358.

(23) Ni, Z.; Masel, R. I. *J. Am. Chem. Soc.* **2006**, *128* (38), 12394.

(24) Li, Z.-Q.; Qiu, L.-G.; Xu, T.; Wu, Y.; Wang, W.; Wu, Z.-Y.; Jiang, X. *Mater. Lett.* **2009**, *63* (1), 78.

(25) Cravillon, J.; Munzer, S.; Lohmeier, S.-J.; Feldhoff, A.; Huber, K.; Wiebcke, M. *Chem. Mater.* **2009**, *21* (8), 1410.

(26) Venna, S. R.; Jasinski, J. B.; Carreon, M. A. *J. Am. Chem. Soc.* **2010**, *132* (51), 18030.

(27) Pan, Y.; Liu, Y.; Zeng, G.; Zhao, L.; Lai, Z. *Chem. Commun.* **2011**, *47* (7), 2071.

(28) Peng, X.; Manna, L.; Yang, W.; Wickham, J.; Scher, E.; Kadavanich, A.; Alivisatos, A. P. *Nature* **2000**, *404* (6773), 59.

(29) Manna, L.; Milliron, D. J.; Meisel, A.; Scher, E. C.; Alivisatos, A. P. *Nat. Mater.* **2003**, *2* (6), 382.

(30) Hermes, S.; Witte, T.; Hikov, T.; Zacher, D.; Bahnmüller, S.; Langstein, G.; Huber, K.; Fischer, R. A. *J. Am. Chem. Soc.* **2007**, *129* (17), 5324.

(31) Tsuruoka, T.; Furukawa, S.; Takashima, Y.; Yoshida, K.; Isoda, S.; Kitagawa, S. *Angew. Chem., Int. Ed.* **2009**, *48* (26), 4739.

(32) Guo, H.; Zhu, Y.; Qiu, S.; Lercher, J. A.; Zhang, H. *Adv. Mater.* **2010**, *22* (37), 4190.

(33) Horcajada, P.; Serre, C.; Grosso, D.; Boissière, C.; Perruchas, S.; Sanchez, C.; Férey, G. *Adv. Mater.* **2009**, *21* (19), 1931.

(34) Schaate, A.; Roy, P.; Godt, A.; Lippke, J.; Waltz, F.; Wiebcke, M.; Behrens, P. *Chem.–Eur. J.* **2011**, *17* (24), 6643.

(35) Cravillon, J.; Nayuk, R.; Springer, S.; Feldhoff, A.; Huber, K.; Wiebcke, M. *Chem. Mater.* **2011**, *23* (8), 2130.

(36) Diring, S.; Furukawa, S.; Takashima, Y.; Tsuruoka, T.; Kitagawa, S. *Chem. Mater.* **2010**, *22* (16), 4531.

(37) Guo, X.; Zhu, G.; Li, Z.; Sun, F.; Yang, Z.; Qiu, S. *Chem. Commun.* **2006**, *30*, 3172.

(38) Zacher, D.; Liu, J.; Huber, K.; Fischer, R. A. *Chem. Commun.* **2009**, *9*, 1031.

(39) Yaghi, O. M.; Li, H.; Groy, T. L. *J. Am. Chem. Soc.* **1996**, *118* (38), 9096.

(40) Lyszczek, R. *J. Therm. Anal. Calorim.* **2008**, *91* (2), 595.

(41) Huang, L.; Wang, H.; Chen, J.; Wang, Z.; Sun, J.; Zhao, D.; Yan, Y. *Microporous Mesoporous Mater.* **2003**, *58* (2), 105.